

Model Predictive Current Control for PMSM Drives With Parameter Robustness Improvement

Xiaoguang Zhang , Member, IEEE, Liang Zhang, and Yongchang Zhang, Senior Member, IEEE

Abstract—In order to solve the parameter dependence problem in model predictive control, an improved model predictive current control (MPCC) method based on the incremental model for surface-mounted permanent-magnet synchronous motor drives is proposed in this paper. First, the parameter sensitivity of a conventional MPCC method is analyzed, which indicates that the parameter mismatches would cause prediction current error and inaccurate delay compensation. Therefore, an incremental prediction model is introduced in this paper to eliminate the use of permanent magnetic flux linkage in a prediction model. Among the parameter of the incremental prediction model, only inductance mismatch contributes to the prediction error, since the influence of resistance mismatch on the control performance is very small. Therefore, in order to improve the antiparameter-disturbance capability of the MPCC method, an inductance disturbance controller, which includes the inductance disturbance observer and inductance extraction algorithm, is presented to update accurate inductance information for the whole control system in real time. Finally, simulation and experimental results both show that the proposed method can effectively eliminate the influence of the parameter mismatches on the control performance and reduce the parameter sensitivity of the MPCC method.

Index Terms—Model predictive current control (MPCC), parameter mismatch, surface-mounted permanent-magnet synchronous motor (SPMSM).

I. INTRODUCTION

IN RECENT years, permanent-magnet synchronous motor (PMSM) is widely used in industrial application due to its high precision, high efficiency, and excellent control performance. However, PMSM system is a typical nonlinear control system, in which the linear current control method, such as proportional-integral (PI) control, is difficult to obtain satisfactory control performance. Therefore, some new control methods have been proposed and applied in PMSM control system,

Manuscript received January 6, 2018; revised March 27, 2018; accepted May 4, 2018. Date of publication May 16, 2018; date of current version December 7, 2018. This work was supported in part by the Beijing Natural Science Foundation under Grant 3172011, in part by the National Natural Science Foundation of China under Grant 51507004, and in part by the Yuyou Talent Project of North China University of Technology. Recommended for publication by Associate Editor I. Slama-Belkhodja. (*Corresponding author: Xiaoguang Zhang*)

The authors are with the Inverter Technologies Engineering Research Center of Beijing, North China University of Technology, Beijing 100144, China, with the Collaborative Innovation Center of Key Power Energy-Saving Technologies in Beijing, Beijing 100144, China, and also with the Collaborative Innovation Center of Electric Vehicles in Beijing, Beijing 100144, China (e-mail: zgx@ncut.edu.cn; wang-kq@qq.com; zyc@ncut.edu.cn).

Color versions of one or more of the figures in this paper are available online at <http://ieeexplore.ieee.org>.

Digital Object Identifier 10.1109/TPEL.2018.2835835

such as fuzzy control, robust control, sliding-mode control, and model predictive control (MPC) [1], [2].

Among these advanced control methods, the MPC receives increased attention because of its simple implementation, straightforward handling of nonlinearities and constraints, and good dynamic performance [3]–[8]. MPC was originally studied and applied in the process industry [9]. However, along with the development of the digital microprocessor, MPC has been widely applied to other application areas, such as power quality [10], [11], machine drive [12]–[14], grid-connected converters [15], [16], and controllable power supplies [17], [18]. In these applications, many research results have been obtained. In order to improve the steady-state control performance of the MPC, the duty-cycle control in direct torque control, which includes two voltage vectors in a control period, is introduced, and the high-performance control is achieved under the condition of no influence on the dynamic response [19]. In the predictive torque control, in order to eliminate the influence of weighting factor on the control performance and solve the problem of lack of theoretical design procedure, some solutions have been proposed, such as multiobjective ranking method [20], fuzzy decision-making strategy [21], empirical procedure approach [22], and voltage tracking error method [23]. Additionally, in the application of multistep prediction system and multilevel conversion system, the computational burden of MPC algorithm would increase exponentially. Therefore, it becomes a key problem to reduce the computational burden. In order to solve this problem, some methods have been presented, such as sphere decoding algorithm [24], [25], the binary search tree method [26].

Although the MPC has gained remarkable research progress, the challenge of strong dependence on system model still needs to be addressed. In an MPC method, the behavior of machine at next control period is predicted according to the machine discrete model. It means that motor parameter in the model is crucial to the prediction performance. Unfortunately, these parameters are not able to remain actual values all the time due to the measurement error or they may change during the operation of the motor. This means that all these parameter mismatches would cause prediction errors of machine control behavior and further deteriorate the control performance of a system [27]. Thus, in order to improve the parameter robustness of predictive control, some methods have been proposed. In [28], a novel predictive current control algorithm is presented to improve the control performance of a system when inductance parameter mismatch exists. In [29], to achieve performance improvement under the condition of system disturbance, a predictive current

control method based on the Luenberger observer is proposed, which more focus on converter uncertainty than model parameter. An improved predictive current controller is presented in [30], which is able to increase robustness to load parameter mismatch. In [31], an improved predictive direct power control method for grid-connected three-phase voltage source converters is presented, which can avoid the influence of inductance variation. These methods mainly focus on the influence of separate parameter mismatch on the predictive control. However, in general, the parameter mismatches, including resistance mismatch, inductance mismatch, and permanent-magnet (PM) flux-linkage mismatch, coexist in the system model. Therefore, it is very necessary to develop predictive control method, which is able to achieve simultaneous suppression of all model parameter mismatches. In [32], a deadbeat current predictive control that can suppress all parameter disturbances is proposed. Although the parameter sensitivity of the PMSM drives can be reduced effectively in this method, the complex design of two observers is inevitable. On the other hand, the model-free MPC methods can be used to eliminate all model parameters [33], [34]. This method adopts measured currents to implement motor behavior prediction, in which the dependence of MPC on model parameter is transferred to the dependence on the accuracy of the current measurement.

In this paper, a simple parameter-robustness-improvement method of MPC for PMSM drives is proposed. First, the prediction errors caused by parameter mismatches (resistance, inductance, and PM flux linkage) in prediction model are analyzed theoretically. Then, the incremental prediction model is introducing to eliminate the use of PM flux-linkage parameter. Additionally, the influences of resistance and inductance mismatch in the incremental model on predictive performance are investigated for the first time in this paper, which indicates that the inductance mismatch is the key factor caused prediction error and the resistance influence can be neglected. Thus, an inductance disturbance controller that includes simple disturbance observer and inductance extraction algorithm is proposed to improve parameter robustness of predictive control system. Finally, simulation and experiment results show the validity of the proposed method.

II. CONVENTIONAL MODEL PREDICATIVE CURRENT CONTROL AND PARAMETER SENSITIVITY ANALYSIS

In this section, the conventional model predictive current control (MPCC) method is introduced briefly, and the parameter sensitivities of the conventional MPCC method are analyzed when the parameter mismatches exist.

A. PMSM Mathematical Model

The dynamical model of a PMSM in synchronous rotating reference frame is given by

$$\begin{cases} u_d = R i_d + L \frac{d i_d}{d t} - \omega_e L i_q \\ u_q = R i_q + L \frac{d i_q}{d t} + \omega_e L i_d + \omega_e \psi_f \end{cases} \quad (1)$$

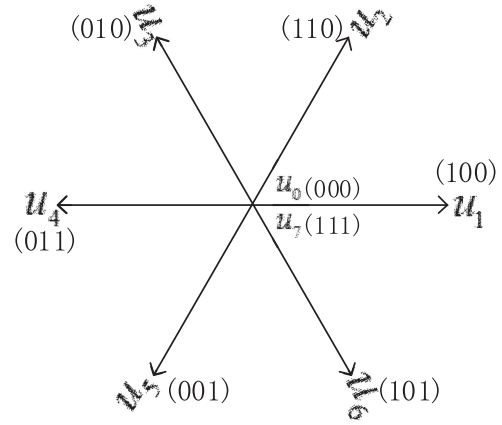


Fig. 1. Basic voltage vector of a two-level inverter.

where u_d and u_q represent the dq -axes voltages; i_d and i_q are the dq -axes currents; ω_e is the electrical rotor speed (rad/s); ψ_f is the PM flux linkage; and R is the winding resistance. Since SPMSM is used in this paper, the cross-axes inductance and the straight-axes inductance are approximately equal, i.e., $L = L_d = L_q$.

According to model (1), the currents at the next instant [$i_d(k+1)$ and $i_q(k+1)$] are able to be predicted using the forward Euler discretization equation as

$$\begin{cases} i_d(k+1) = \left(1 - \frac{TR}{L}\right) \cdot i_d(k) + T\omega_e i_q(k) + \frac{T}{L} \cdot u_d(k) \\ i_q(k+1) = \left(1 - \frac{TR}{L}\right) \cdot i_q(k) - T\omega_e i_d(k) + \frac{T}{L} \cdot u_q(k) \\ \quad - \frac{T\omega_e \psi_f}{L} \end{cases} \quad (2)$$

where T represents a control period.

B. MPCC Method

For a two-level three-phase inverter, the basic voltage vector consists of six nonzero vectors (u_1, u_2, \dots, u_6) and two zero vectors (u_0 and u_7), as shown in Fig. 1. Therefore, based on the current prediction equation (2), the current value at the $(k+1)$ th instant under different basic voltage vectors can be predicted. Then, prediction current values are substituted into the cost function (3). The voltage vector that has the minimum value of the cost function is selected as the optimal voltage vector, and is applied to the motor by the inverter

$$g = |i_d^* - i_d| + |i_q^* - i_q| \quad (3)$$

where i_d^* and i_q^* are the d -axis and q -axis currents commands, respectively, and i_d^* is set to zero and i_q^* is obtained from the output of a speed loop.

Additionally, it is worth to highlight that the calculation delay is unavoidable due to the digital implementation mode of the prediction control. It means that the optimal voltage

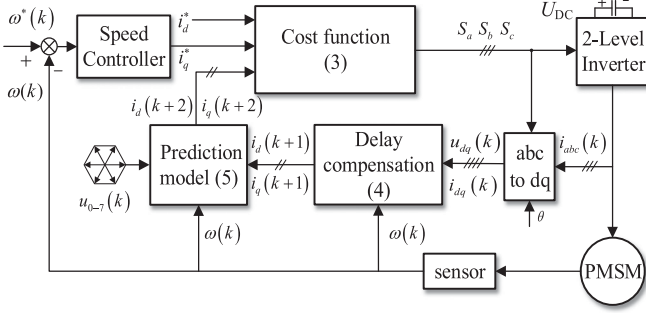


Fig. 2. Control diagram of a conventional MPCC method.

vector selected by the cost function at this control period will be applied for the motor at the next control period, which will deteriorate the control performance of the whole control system. Therefore, it is very necessary to compensate one-step calculation delay. Based on the measured currents [$i_d(k)$, $i_q(k)$] and voltages [$u_d(k)$, $u_q(k)$], the delay compensated currents can be obtained according to the prediction model (2) as

$$\begin{cases} i_d^p(k+1) = \left(1 - \frac{TR}{L}\right) \cdot i_d(k) + T\omega_e i_q(k) + \frac{T}{L} \cdot u_d(k) \\ i_q^p(k+1) = \left(1 - \frac{TR}{L}\right) \cdot i_q(k) - T\omega_e i_d(k) + \frac{T}{L} \cdot u_q(k) \\ \quad - \frac{T\omega_e \psi_f}{L}. \end{cases} \quad (4)$$

These compensated currents $i_d^p(k+1)$ and $i_q^p(k+1)$ are employed to replace the measured currents $i_d(k)$ and $i_q(k)$ of the model (2), which means that the current prediction model (2) can be updated after the one-step delay compensation as

$$\begin{cases} i_d(k+2) = \left(1 - \frac{TR}{L}\right) \cdot i_d^p(k+1) + T\omega_e i_q^p(k+1) \\ \quad + \frac{T}{L} \cdot u_d(k+1) \\ i_q(k+2) = \left(1 - \frac{TR}{L}\right) \cdot i_q^p(k+1) - T\omega_e i_d^p(k+1) \\ \quad + \frac{T}{L} \cdot u_q(k+1) - \frac{T\omega_e \psi_f}{L}. \end{cases} \quad (5)$$

The principle of the conventional MPCC method is shown in Fig. 2.

C. Parameter Sensitivity Analysis of the MPCC Method

The MPCC is a kind of model-based control method due to the existence of three machine parameters (resistance R , inductance L , and PM flux linkage ψ_f) in a current prediction model. This means that MPCC is parameter sensitive, and the accuracy of the prediction model will directly influence the control performance of the whole system. In order to evaluate how the MPCC is

sensitive to a parameter mismatch, parameter sensitivity analysis is discussed in this section.

According to the current prediction model (2), when the parameter mismatch exists, the current prediction model can be expressed as

$$\begin{cases} i'_d(k+1) = \left[1 - \frac{T(R + \Delta R)}{(L + \Delta L)}\right] \cdot i_d(k) + T\omega_e i_q(k) \\ \quad + \frac{T}{(L + \Delta L)} \cdot u_d(k) \\ i'_q(k+1) = \left[1 - \frac{T(R + \Delta R)}{(L + \Delta L)}\right] \cdot i_q(k) - T\omega_e i_d(k) \\ \quad + \frac{T}{(L + \Delta L)} \cdot u_q(k) - \frac{T\omega_e(\psi_f + \Delta\psi_f)}{(L + \Delta L)} \end{cases} \quad (6)$$

where ΔR , ΔL , and $\Delta\psi_f$ are parameter errors between the parameter values and the true values. Then, the prediction errors between the error-free model (2) and model (6) subjected to parameter variation can be obtained as

$$\begin{cases} E_d = i'_d(k+1) - i_d(k+1) = \frac{TR\Delta L - T\Delta RL}{L(L + \Delta L)} \cdot i_d(k) \\ \quad - \frac{T\Delta L}{L(L + \Delta L)} \cdot u_d(k) \\ E_q = i'_q(k+1) - i_q(k+1) = \frac{TR\Delta L - T\Delta RL}{L(L + \Delta L)} \cdot i_q(k) \\ \quad - \frac{T\Delta L}{L(L + \Delta L)} \cdot u_q(k) + \frac{T\omega_e\psi_f\Delta L - T\omega_e\Delta\psi_f L}{L(L + \Delta L)}. \end{cases} \quad (7)$$

Equation (7) implies that the mismatch or uncertainty of any one parameter will lead to the error of the prediction current. Fig. 3 shows the relationship between the prediction error and the parameter mismatches. It can be seen that the parameter mismatch of inductance and PM flux linkage has a great influence on the prediction error; however, the influence caused by the resistance mismatch is small.

Additionally, in general, one-step delay should be compensated based on (4) in real application. However, due to the existence of the parameter mismatch, the delay compensation equation (4) has a different form, which is able to be expressed using accurate currents and prediction errors, shown as

$$\begin{cases} i_d^p(k+1) = i_d(k+1) + E_d \\ i_q^p(k+1) = i_q(k+1) + E_q. \end{cases} \quad (8)$$

The compensated currents $i_d^p(k+1)$ and $i_q^p(k+1)$ both are not accurate values of the next instant due to the existence of parameter mismatch. Then, under the condition of the parameter mismatch, the prediction currents after inaccurate delay

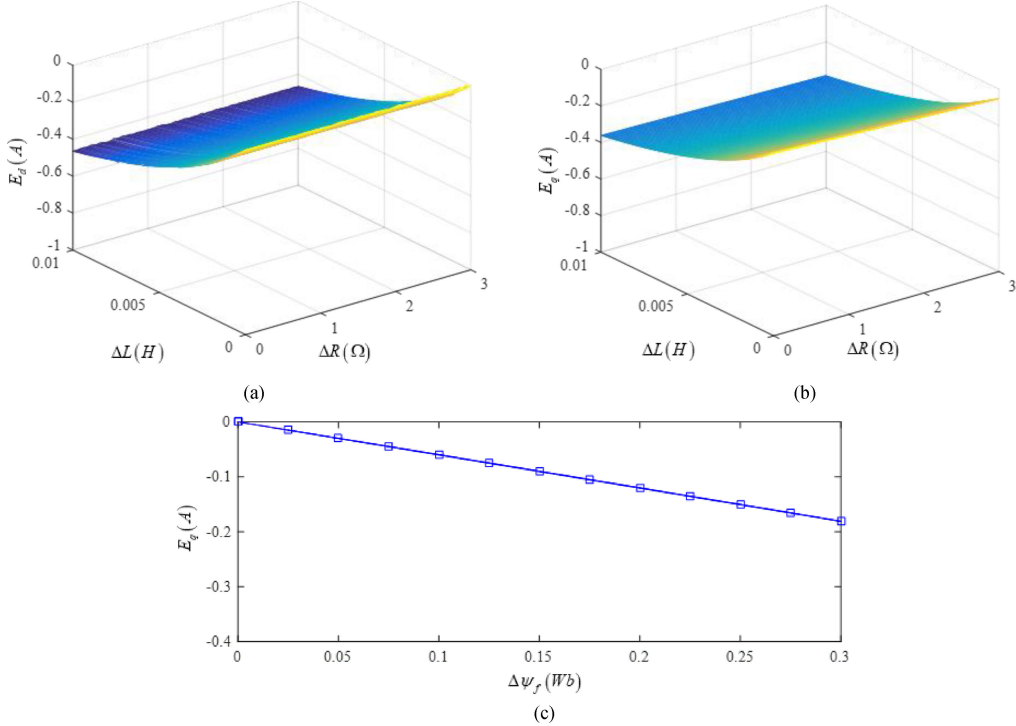


Fig. 3. Conventional MPCC current prediction errors without one-step delay compensation under the condition of 500 r/min and 3 N·m. (a) Relationship between d -axis current error and the mismatch of resistance and inductance. (b) Relationship between q -axis current error and the mismatch of resistance and inductance. (c) Relationship between q -axis current error and flux-linkage mismatch.

compensation can be derived as

$$\left\{ \begin{array}{l} i'_d(k+2) = \left[1 - \frac{T(R+\Delta R)}{(L+\Delta L)} \right] \cdot [i_d(k+1) + E_d] \\ \quad + T\omega_e [i_q(k+1) + E_q] + \frac{T}{(L+\Delta L)} \cdot u_d(k+1) \\ i'_q(k+2) = \left[1 - \frac{T(R+\Delta R)}{(L+\Delta L)} \right] \cdot [i_q(k+1) + E_q] \\ \quad - T\omega_e [i_d(k+1) + E_d] + \frac{T}{(L+\Delta L)} \\ \quad \cdot u_q(k+1) - \frac{T\omega_e(\psi_f + \Delta\psi_f)}{(L+\Delta L)}. \end{array} \right. \quad (9)$$

Similarly, the prediction errors can be obtained by subtracting model (5) from (9) as

$$\left\{ \begin{array}{l} E_d^{\text{comp}} = \left[1 - \frac{T(R+\Delta R)}{(L+\Delta L)} \right] \cdot E_d + \frac{TR\Delta L - T\Delta RL}{L(L+\Delta L)} \\ \quad \cdot i_d(k+1) + T\omega_e E_q - \frac{T\Delta L}{L(L+\Delta L)} \cdot u_d(k+1) \\ E_q^{\text{comp}} = \left[1 - \frac{T(R+\Delta R)}{(L+\Delta L)} \right] \cdot E_q + \frac{TR\Delta L - T\Delta RL}{L(L+\Delta L)} \\ \quad \cdot i_q(k+1) - T\omega_e E_d - \frac{T\Delta L}{L(L+\Delta L)} \cdot u_q(k+1) \\ \quad + \frac{T\omega_e\psi_f\Delta L - T\omega_e\Delta\psi_f L}{L(L+\Delta L)} \end{array} \right. \quad (10)$$

where E_d^{comp} and E_q^{comp} represent prediction errors after one-step delay compensation. Equation (10) implies that the prediction error is further expanded after one-step delay compensation. Fig. 4 shows the relationship between the prediction errors and different degrees of uncertainty in the parameters under the condition of one-step delay compensation. Through comparison between Figs. 3 and 4, it can be seen that the prediction error caused by the parameter mismatch when one-step delay compensation is considered is larger than that without one-step delay compensation. These comparison results are consistent with the theoretical analysis. Therefore, in order to avoid deteriorating the control performance of MPC caused by parameter mismatches and delay compensation, it is necessary to develop a strong parameter-robustness-control algorithm.

III. PRINCIPLE OF THE PROPOSED METHOD

To improve the control performance under inductance parameter disturbance, an improved MPCC method is proposed in this paper. The schematic block diagram of the proposed method is shown in Fig. 5, which mainly includes the following parts: incremental prediction model, delay compensation, inductance disturbance controller (including inductance disturbance observer and inductance extraction algorithm), and cost-function-based vector selection. In addition, the current reference i_q^* is obtained by the output of speed PI regulator. The details of this method will be elaborated in the following section.

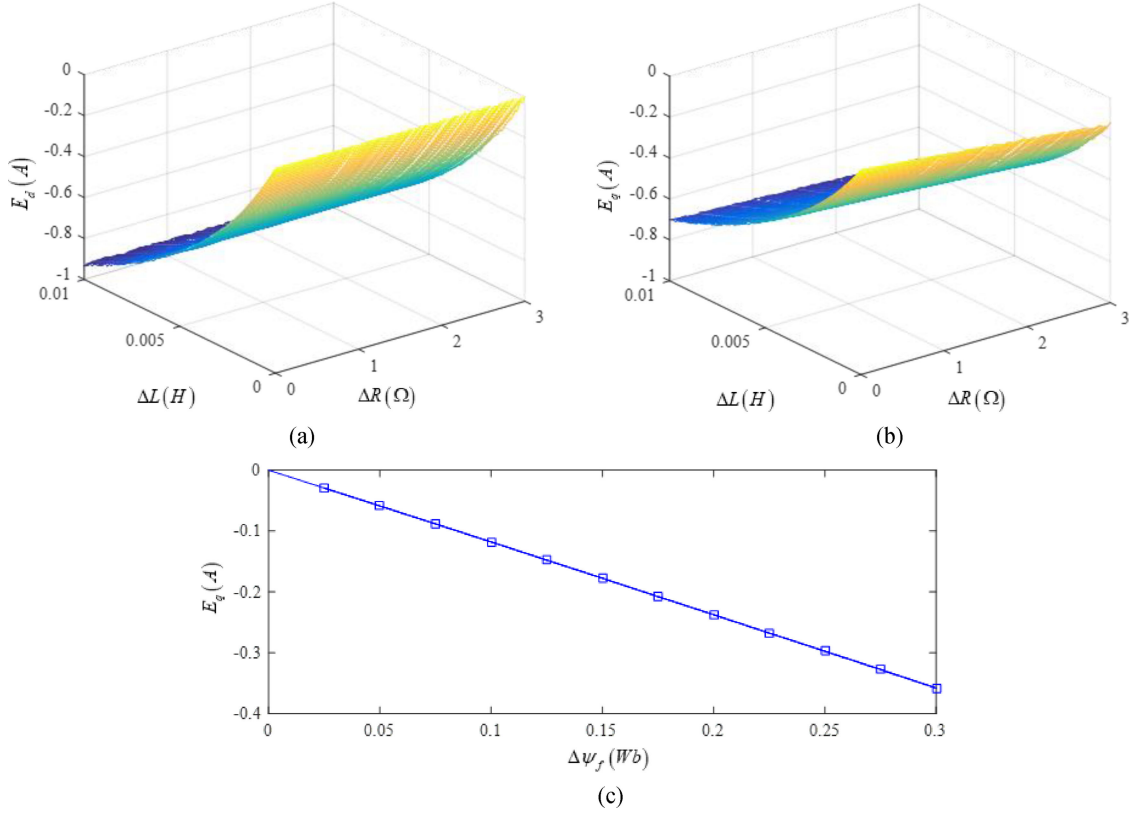


Fig. 4. Conventional MPCC current prediction error with one-step delay compensation under the condition of 500 r/min and 3 N·m. (a) Relationship between d -axis current error and the mismatch of resistance and inductance. (b) Relationship between q -axis current error and the mismatch of resistance and inductance. (c) Relationship between q -axis current error and flux-linkage mismatch.

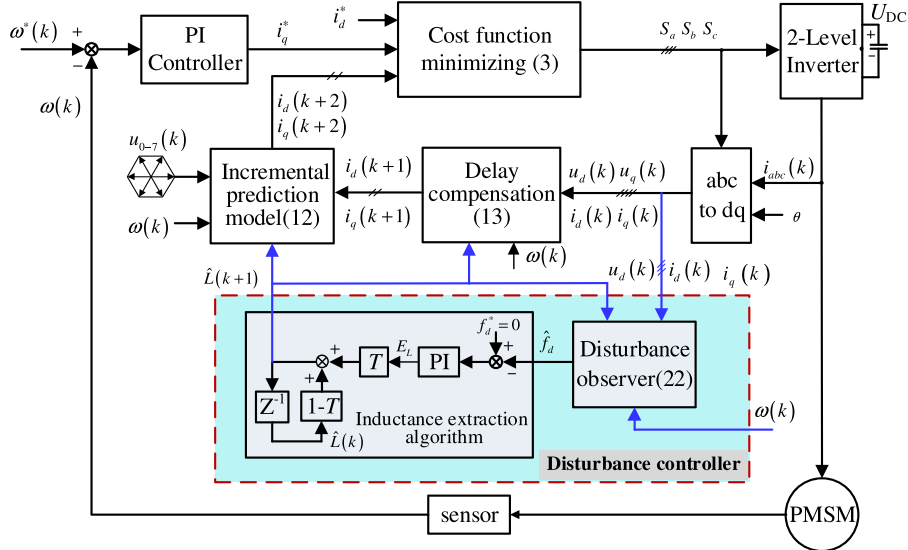


Fig. 5. Control diagram of the proposed MPCC method.

A. Incremental Prediction Model

1) *Elimination of the PM Flux Linkage:* The above analysis shows that any parameter mismatch will lead to the prediction error and affect the control performance of MPCC method. Consequently, in order to eliminate the influence of the PM flux

linkage, an incremental prediction model is introduced in this paper. Differed from the conventional prediction model, an incremental model predicts current based on two different instant.

It is known that the currents at $(k + 1)$ th instant can be predicted according to (2); similarly, the currents at (k) th instant

can be expressed as

$$\begin{cases} i_d(k) = \left(1 - \frac{TR}{L}\right) \cdot i_d(k-1) + T\omega_e i_q(k-1) \\ \quad + \frac{T}{L} \cdot u_d(k-1) \\ i_q(k) = \left(1 - \frac{TR}{L}\right) \cdot i_q(k-1) - T\omega_e i_d(k-1) \\ \quad + \frac{T}{L} \cdot u_q(k-1) - \frac{T\omega_e \psi_f}{L}. \end{cases} \quad (11)$$

Subtracting (11) from (2), the incremental prediction model can be obtained as

$$\begin{cases} i_d(k+1) = \left(2 - \frac{TR}{L}\right) \cdot i_d(k) - \left(1 - \frac{TR}{L}\right) \cdot i_d(k-1) \\ \quad + T\omega [i_q(k) - i_q(k-1)] \\ \quad + \frac{T}{L} \cdot [u_d(k) - u_d(k-1)] \\ i_q(k+1) = \left(2 - \frac{TR}{L}\right) \cdot i_q(k) - \left(1 - \frac{TR}{L}\right) \cdot i_q(k-1) \\ \quad - T\omega [i_d(k) - i_d(k-1)] \\ \quad + \frac{T}{L} \cdot [u_q(k) - u_q(k-1)]. \end{cases} \quad (12)$$

From (12), it can be seen that the PM flux linkage in the conventional prediction model is eliminated. It means that the flux-linkage parameter mismatch has no influence on the predicted current and the control performance of the whole system.

Similar to the one-step delay compensation in the conventional MPCC, compensated incremental prediction model can be expressed as

$$\begin{cases} i_d(k+2) = \left(2 - \frac{TR}{L}\right) \cdot i_d^p(k+1) - \left(1 - \frac{TR}{L}\right) \\ \quad \cdot i_d^p(k) + T\omega [i_q^p(k+1) - i_q^p(k)] \\ \quad + \frac{T}{L} \cdot [u_d(k+1) - u_d(k)] \\ i_q(k+2) = \left(2 - \frac{TR}{L}\right) \cdot i_q^p(k+1) - \left(1 - \frac{TR}{L}\right) \\ \quad \cdot i_q^p(k) - T\omega [i_d^p(k+1) - i_d^p(k)] \\ \quad + \frac{T}{L} \cdot [u_q(k+1) - u_q(k)] \end{cases} \quad (13)$$

where $i_d^p(k+1)$ and $i_q^p(k+1)$ represent one-step delay compensation currents at $(k+1)$ th instant, which are calculated according to (4). In addition, $i_d^p(k)$ and $i_q^p(k)$ represent measured currents at (k) th instant.

2) Parametric Sensitivity Analysis of the Incremental Prediction Model: Even though an incremental prediction model eliminates the parameter of PM flux linkage, resistance R and inductance L still exist in the model. In order to evaluate the influence of resistance and inductance mismatch, the parameter sensitivity of the incremental model is analyzed in this section.

According to the incremental prediction model (12), when the parameter mismatch exists, the current prediction model can be expressed as

$$\begin{cases} i'_d(k+1) = \left[2 - \frac{T(R + \Delta R)}{(L + \Delta L)}\right] \cdot i_d(k) - \left[1 - \frac{T(R + \Delta R)}{(L + \Delta L)}\right] \\ \quad \cdot i_d(k-1) + T\omega [i_q(k) - i_q(k-1)] \\ \quad + \frac{T}{(L + \Delta L)} \cdot [u_d(k) - u_d(k-1)] \\ i'_q(k+1) = \left[2 - \frac{T(R + \Delta R)}{(L + \Delta L)}\right] \cdot i_q(k) - \left[1 - \frac{T(R + \Delta R)}{(L + \Delta L)}\right] \\ \quad \cdot i_q(k-1) - T\omega [i_d(k) - i_d(k-1)] \\ \quad + \frac{T}{(L + \Delta L)} \cdot [u_q(k) - u_q(k-1)]. \end{cases} \quad (14)$$

Then, the prediction errors between the error-free incremental model (12) and model (14) subjected to parameter mismatch can be obtained as

$$\begin{cases} D_d = \frac{TR\Delta L - T\Delta RL}{L(L + \Delta L)} \cdot [i_d(k) - i_d(k-1)] - \frac{T\Delta L}{L(L + \Delta L)} \\ \quad \cdot [u_d(k) - u_d(k-1)] \\ D_q = \frac{TR\Delta L - T\Delta RL}{L(L + \Delta L)} \cdot [i_q(k) - i_q(k-1)] - \frac{T\Delta L}{L(L + \Delta L)} \\ \quad \cdot [u_q(k) - u_q(k-1)] \end{cases} \quad (15)$$

where D_d and D_q represent the current prediction errors of the d -axis and the q -axis, respectively. From (15), it is seen that not only the parameter uncertainties but also the instant current and voltage at different instant have an effect on the prediction error. However, it should be noted that when the motor operates at the steady state, which means that d -axis and q -axis currents satisfy $i_d(k) = i_d(k-1)$ and $i_q(k) = i_q(k-1)$, prediction errors (15) can be simplified as

$$\begin{cases} D_d = -\frac{T\Delta L}{L(L + \Delta L)} \cdot [u_d(k) - u_d(k-1)] \\ D_q = -\frac{T\Delta L}{L(L + \Delta L)} \cdot [u_q(k) - u_q(k-1)]. \end{cases} \quad (16)$$

Equation (16) implies that under the condition of the steady state, resistance mismatch has no influence on the prediction error, and only inductance mismatch contributes to the prediction error.

Additionally, similar to (8), when one-step delay compensation is considered, compensated currents can be expressed by accurate currents and prediction errors, thus the incremental prediction model under the condition of the parameter mismatch is

modified as

$$\left\{ \begin{array}{l} i'_d(k+2) = \left[2 - \frac{T(R + \Delta R)}{(L + \Delta L)} \right] \cdot [i_d(k+1) + D_d] \\ \quad + \left[1 - \frac{T(R + \Delta R)}{(L + \Delta L)} \right] \cdot i_d^p(k) \\ \quad + T\omega [i_q(k+1) + D_q - i_q^p(k)] + \frac{T}{(L + \Delta L)} \\ \quad \cdot [u_d(k+1) - u_d(k)] \\ \\ i'_q(k+2) = \left[2 - \frac{T(R + \Delta R)}{(L + \Delta L)} \right] \cdot [i_q(k+1) + D_q] \\ \quad - \left[1 - \frac{T(R + \Delta R)}{(L + \Delta L)} \right] \cdot i_q^p(k) \\ \quad - T\omega [i_d(k+1) + D_d - i_d^p(k)] + \frac{T}{(L + \Delta L)} \\ \quad \cdot [u_q(k+1) - u_q(k)]. \end{array} \right. \quad (17)$$

Similarly, the prediction errors can be obtained by subtracting the error-free model (13) from (17) as

$$\left\{ \begin{array}{l} D_d^{\text{comp}} = \left[2 - \frac{T(R + \Delta R)}{(L + \Delta L)} \right] \cdot D_d + \frac{TR\Delta L - T\Delta RL}{L(L + \Delta L)} \\ \quad \cdot [i_d(k+1) - i_d(k)] + T\omega_e D_q - \frac{T\Delta L}{L(L + \Delta L)} \\ \quad \cdot [u_d(k+1) - u_d(k)] \\ \\ D_q^{\text{comp}} = \left[2 - \frac{T(R + \Delta R)}{(L + \Delta L)} \right] \cdot D_q + \frac{TR\Delta L - T\Delta RL}{L(L + \Delta L)} \\ \quad \cdot [i_q(k+1) - i_q(k)] - T\omega_e D_d - \frac{T\Delta L}{L(L + \Delta L)} \\ \quad \cdot [u_q(k+1) - u_q(k)] \end{array} \right. \quad (18)$$

where D_d^{comp} and D_q^{comp} represent the current prediction errors of the d -axis and the q -axis, respectively, when one-step delay compensation is adopted. The prediction errors (18) can be simplified as (19) at steady state

$$\left\{ \begin{array}{l} D_d^{\text{comp}} = \left[3 - \frac{T(R + \Delta R)}{(L + \Delta L)} \right] \cdot D_d + T\omega_e D_q \\ \\ D_q^{\text{comp}} = \left[3 - \frac{T(R + \Delta R)}{(L + \Delta L)} \right] \cdot D_q - T\omega_e D_d. \end{array} \right. \quad (19)$$

It is obvious that similar to the conventional MPCC, one-step delay compensation in incremental model also enlarge the current prediction error. This increase of the prediction error is mainly caused by the inductance mismatch, since the item $T\Delta R$ in (19) is very small, which can be negligible.

B. Inductance Disturbance Controller

In order to suppress the influence of the inductance mismatch on the control performance, an inductance disturbance controller, including inductance disturbance observer and inductance extraction algorithm, is proposed in this paper. First, based on extend sliding-mode observation theory, the inductance

disturbance observer is designed to observe the parameter disturbance caused by the inductance mismatch in real time. This observed disturbance includes the actual inductance information. Therefore, the inductance extraction algorithm is presented to extract motor inductance form the parameter disturbance. Based on the extracted actual inductance, the accurate prediction model can be obtained and the tracking error caused by the inductance mismatch can be eliminated.

1) *Design of an Inductance Disturbance Observer:* Based on motor model (1), when the inductance parameter mismatch is taken into accounts, a d -axis voltage equation of PMSM can be described as follows:

$$\left\{ \begin{array}{l} u_d = L \frac{di_d}{dt} + Ri_d - \omega_e Li_q + f_d \\ \frac{df_d}{dt} = F_d. \end{array} \right. \quad (20)$$

In (20), u_d represents the measured voltage and f_d represents the inductance parameter disturbance which is expressed as (21), and F_d is the variation rate of the disturbance f_d

$$f_d = \Delta L \cdot \frac{di_d}{dt} - \Delta L \omega_e \cdot i_q. \quad (21)$$

According to (21), it is obvious that inductance information is included in inductance disturbance f_d .

Based on (20), a sliding-mode disturbance observer is designed as

$$\left\{ \begin{array}{l} u_d = L \frac{\hat{d}\hat{i}_d}{dt} + R\hat{i}_d - \omega_e Li_q + \hat{f}_d + D_{dsmo} \\ \frac{d\hat{f}_d}{dt} = G_d D_{dsmo} \end{array} \right. \quad (22)$$

where \hat{i}_d and \hat{f}_d represent the estimated values of the d -axis current and the disturbance, respectively; coefficient G_d represents the sliding-mode control gain, and D_{dsmo} represents the sliding-mode function, which is designed in the following section.

Next, subtracting (20) from (22), the error equation can be obtained as

$$\left\{ \begin{array}{l} \frac{de_1}{dt} = -\frac{R}{L}e_1 - \frac{1}{L}e_2 - \frac{1}{L}D_{dsmo} \\ \frac{de_2}{dt} = G_d D_{dsmo} - F_d \end{array} \right. \quad (23)$$

where $e_1 = \hat{i}_d - i_d$ is the estimation error of the d -axis current, and $e_2 = \hat{f}_d - f_d$ is the disturbance estimation error.

Sliding-mode control function D_{dsmo} , in this paper, should be reasonably designed to ensure the fast convergence of errors e_1 and e_2 . Therefore, reaching-law-based sliding-mode design method is employed. First, the estimation error e_1 of the d -axis current is selected as the sliding-mode surface, this means that the sliding-mode surface s satisfies $s = e_1 = \hat{i}_d - i_d$. Then, a simple equal speed reaching law is adopted in this study as

$$\frac{ds}{dt} = -k \cdot \text{sign}(s) \quad (24)$$

where reaching law parameter k is positive.

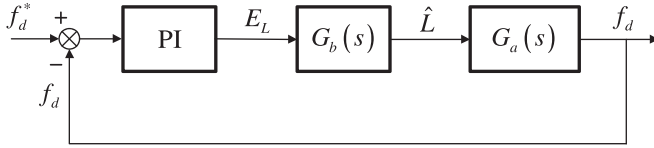


Fig. 6. Block diagram of an inductance extraction system.

Substituting (24) into (23), yields

$$-k \cdot \text{sign}(s) = -\frac{R}{L}e_1 - \frac{1}{L}e_2 - \frac{1}{L}D_{dsmo}. \quad (25)$$

Then, considering e_2 as a disturbance, the sliding-mode control function can be derived as

$$D_{dsmo} = -R \cdot e_1 + k \cdot L \cdot \text{sign}(s). \quad (26)$$

It should be highlighted that the designed sliding-mode control function (26) must satisfy the stability condition of sliding mode, which means that (27) must be satisfied

$$s \cdot \frac{d\dot{s}}{dt} = e_1 \cdot \left(-\frac{R}{L}e_1 - \frac{1}{L}e_2 - \frac{1}{L}D_{dsmo} \right) \leq 0. \quad (27)$$

Substituting (26) into (27), the solution can be obtained as

$$k > \frac{|e_2|}{L}. \quad (28)$$

Therefore, reaching law parameter k should be selected based on (28) to ensure the stability of designed sliding-mode observer. Then, e_1 and its derivative can converge to zero along with the sliding mode occurring, i.e., $e_1 = \frac{de_1}{dt} = 0$. Thus, the error equation (23) can be simplified as

$$\frac{d\dot{e}_2}{dt} + G_d e_2 + F_d = 0. \quad (29)$$

The solution of e_2 is obtained as

$$e_2 = e^{-G_d t} \cdot \left(C + \int F_d \cdot e^{G_d t} dt \right) \quad (30)$$

where C is a constant. From (30), it is obvious that the parameter G_d must be positive to ensure the convergence of error e_2 .

2) Inductance Extraction Algorithm: Based on the designed observer, an inductance extraction algorithm is presented to gain an accurate inductance value from the output of a disturbance observer (estimated disturbance). The control structure of this algorithm is constructed as shown as Fig. 6, in which a PI controller is adopted to adjust estimated inductance. The detailed process is introduced as follows.

Substituting (26) into the second equation of (22) and introducing the estimated inductance, the relationship between the estimated disturbance and estimated inductance in this control system can be obtained as

$$\frac{d\hat{f}_d}{dt} = G_d D_{dsmo} = G_d \cdot \left(-R \cdot e_1 + k \cdot \hat{L} \cdot \text{sign}(s) \right) \quad (31)$$

where \hat{L} is the estimated value of inductance. In the steady state, the error e_1 is equal to zero due to sliding mode occurring, then

TABLE I
PARAMETERS OF AN SPMSM SYSTEM

Parameter	Description	Value
P	Number of pole pairs	2
$R(\Omega)$	Stator resistance	3.18
$L(\text{mH})$	Stator inductance	8.5
$\psi_f (\text{Wb})$	Permanent magnet flux linkage	0.4
$J(\text{kg}\cdot\text{m}^2)$	Rotational inertia	0.00046
$T(\text{N.m})$	Rated torque	6
$V_{DC}(\text{V})$	DC bus voltage	310

(31) is simplified as

$$\frac{d\hat{f}_d}{dt} = G_d D_{dsmo} = G_d \cdot k \cdot \hat{L} \cdot \text{sign}(s). \quad (32)$$

Therefore, the estimated inductance can be expressed as

$$\hat{L} = \begin{cases} \frac{d\hat{f}_d}{dt} \cdot \frac{1}{G_d \cdot k} & (s > 0) \\ -\frac{d\hat{f}_d}{dt} \cdot \frac{1}{G_d \cdot k} & (s < 0) \end{cases} \quad (33)$$

which means

$$\hat{L} = \left| \frac{d\hat{f}_d}{dt} \cdot \frac{1}{G_d \cdot k} \right|. \quad (34)$$

Then, considering disturbance f_d as the output and estimated inductance \hat{L} as the input, the following transfer function can be obtained:

$$G_a(s) = \frac{f_d(s)}{\hat{L}(s)} = \frac{G_d k}{s}. \quad (35)$$

In addition, in this paper, the control function of an estimated inductance is designed as

$$\hat{L}(k+1) = \hat{L}(k) \cdot (1 - T) + T \cdot E_L \quad (36)$$

where $\hat{L}(k)$ and $\hat{L}(k+1)$ represent the estimated inductances at (k) th instant and $(k+1)$ th instant, respectively; E_L is the output of disturbance PI controller, which is designed in the following section. Similarly, according to (36), the transfer function between output \hat{L} and input E_L can be obtained as

$$G_b(s) = \frac{\hat{L}(s)}{E_L(s)} = \frac{1}{s+1}. \quad (37)$$

Then, according to (35), (37) and control structure Fig. 6, the open-loop transfer function of this control system can be obtained as

$$w(s) = \frac{G_d k}{s} \cdot \left(k_p + \frac{k_i}{s} \right) \cdot \frac{1}{s+1}. \quad (38)$$

It can be simplified as a typical type-II system as

$$w(s) = \frac{k_i k G_d \left(\frac{k_p}{k_i} s + 1 \right)}{s^2 (s+1)} \quad (39)$$

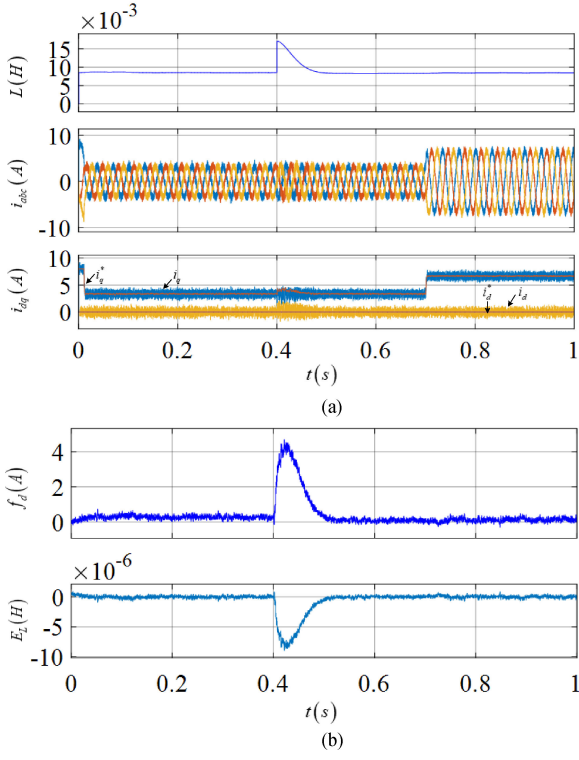


Fig. 7. Simulation results of the proposed MPCC methods with 100% error in inductance. (a) Inductance in the model, phase current, and dq -axes current. (b) Estimated disturbances of observer and the output of PI controller in the inductance extraction algorithm.

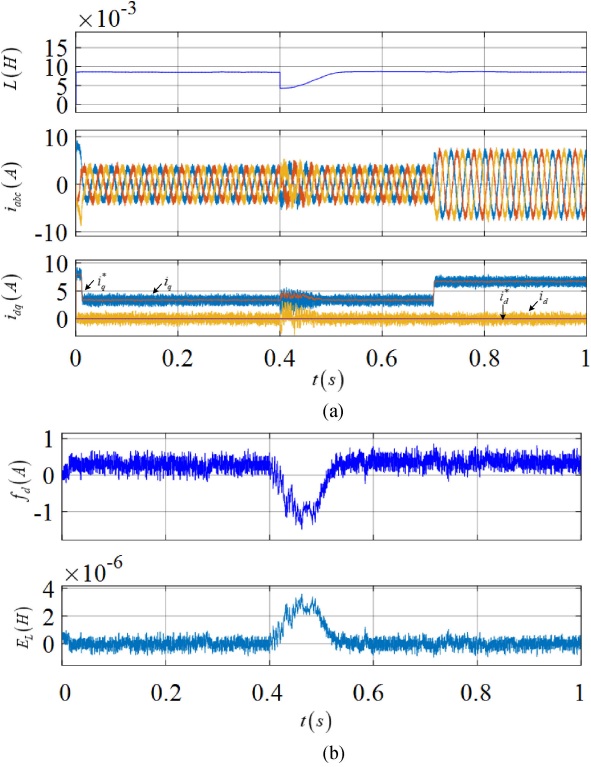


Fig. 8. Simulation results of the proposed MPCC methods with 50% error in inductance. (a) Inductance in the model, phase current, and dq -axes current. (b) Estimated disturbances of observer and the output of PI controller in the inductance extraction algorithm.

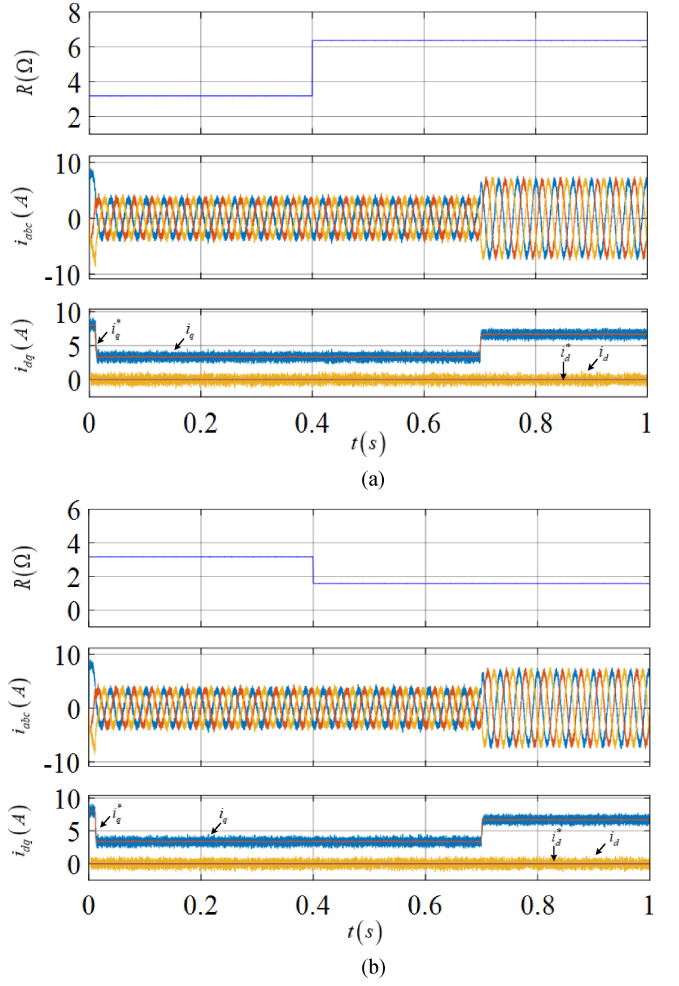


Fig. 9. Simulation results of the proposed MPCC method with different error in resistance. (a) When resistance in the model increases 100%. (b) When inductance in the prediction model decreases 50%.

where k_p and k_i are proportion and integral parameters of the PI controller, respectively. In this paper, the criterion to get minimum peak of amplitude–frequency characteristic is employed to calculate controller parameters k_p and k_i [20]. Therefore, the following relationship expression can be obtained:

$$\begin{cases} h = \frac{k_p}{k_i} \\ k_i k G_d = \frac{h+1}{2h^2} \end{cases} \quad (40)$$

where h represents the intermediate frequency bandwidth, which is related to the dynamic performance of the system. According to paper [21], when the bandwidth $h = 5$, typical type-II system has satisfactory tracking performance and immunity performance. Then, the PI controller parameters can be calculated by

$$\begin{cases} k_p = 5k_i \\ k_i = \frac{0.12}{k G_d}. \end{cases} \quad (41)$$

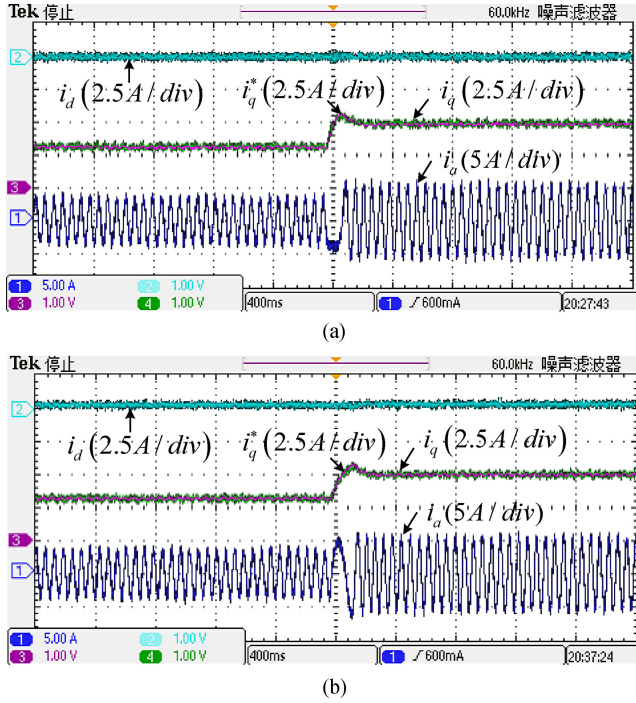


Fig. 10. Experimental results of both methods without the parameter mismatch. (a) Conventional MPCC method. (b) Proposed MPCC method.

Based on the designed control parameters k_p and k_i , the actual inductance value can be obtained easily. Then, the accurate delay compensation can be achieved and the current prediction error caused by the inductance mismatch can be eliminated by updating the actual inductance of incremental prediction model. Therefore, the whole control system can keep its good control performance and antiinterference capability of parameter.

IV. SIMULATION AND EXPERIMENTAL RESULTS

In order to verify the effectiveness of the proposed method, the simulation is carried out in the MATLAB/Simulink environment, and the experimental test is performed on the platform of the TMS320F28335 processor. The sample frequency used in the simulation and experiment is 15 kHz. In addition, PMSM parameters are given in Table I.

The simulation results of the proposed method are shown in Figs. 7–9, when the parameter mismatch and load torque change suddenly occur at 0.4 and 0.7 s, respectively. Fig. 7 depicts the results of system response when inductance in the prediction model increases 100%. On the other hand, when motor inductance in the prediction model decreases 50%, the simulation results are shown in Fig. 8. From Figs. 7 and 8, it can be seen that when the inductance parameter mismatch occurs, the inductance parameter in the model is able to be adjusted to the actual value under the control of the proposed method. Along with the inductance value is modified, the observed parameter disturbance f_d also converges to zero. Additionally, at 0.7 s, the load torque is increased from 50% rated value to 100% rated value. It is obvious that the sudden change of the load torque has no influence on the inductance value, which shows

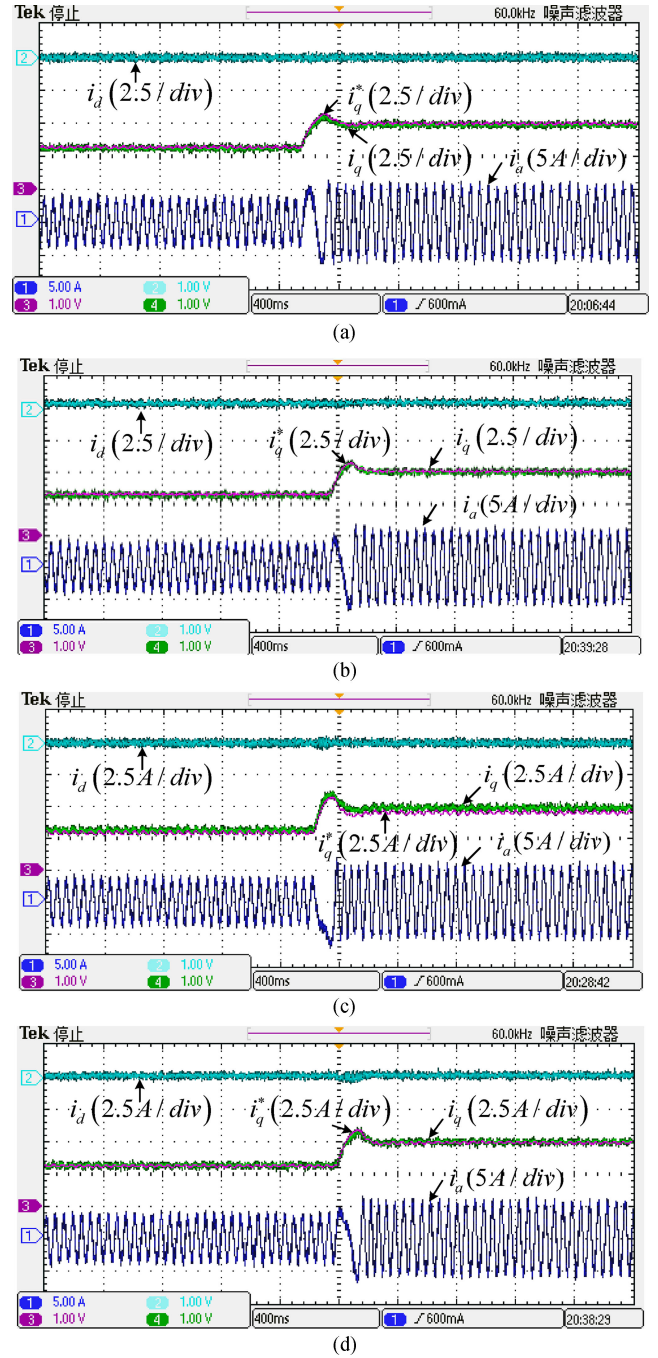


Fig. 11. Experimental results of both methods with the resistance parameter mismatch. (a) Reference and response of dq -axes current and phase current under conventional MPCC (50% error in resistance). (b) Reference and response of dq -axes current and phase current under the proposed MPCC method (50% error in resistance). (c) Reference and response of dq -axes current and phase current under conventional MPCC (100% error in resistance). (d) Reference and response of dq -axes current and phase current under the proposed MPCC method (100% error in resistance).

the good antidiisturbance capability of the proposed method. Fig. 9 shows the simulation results of the proposed method with different resistance mismatches. It can be seen that the influence of the resistance mismatch on the control performance is very small and almost negligible, which further prove that consistency between simulation results and theoretical analysis.

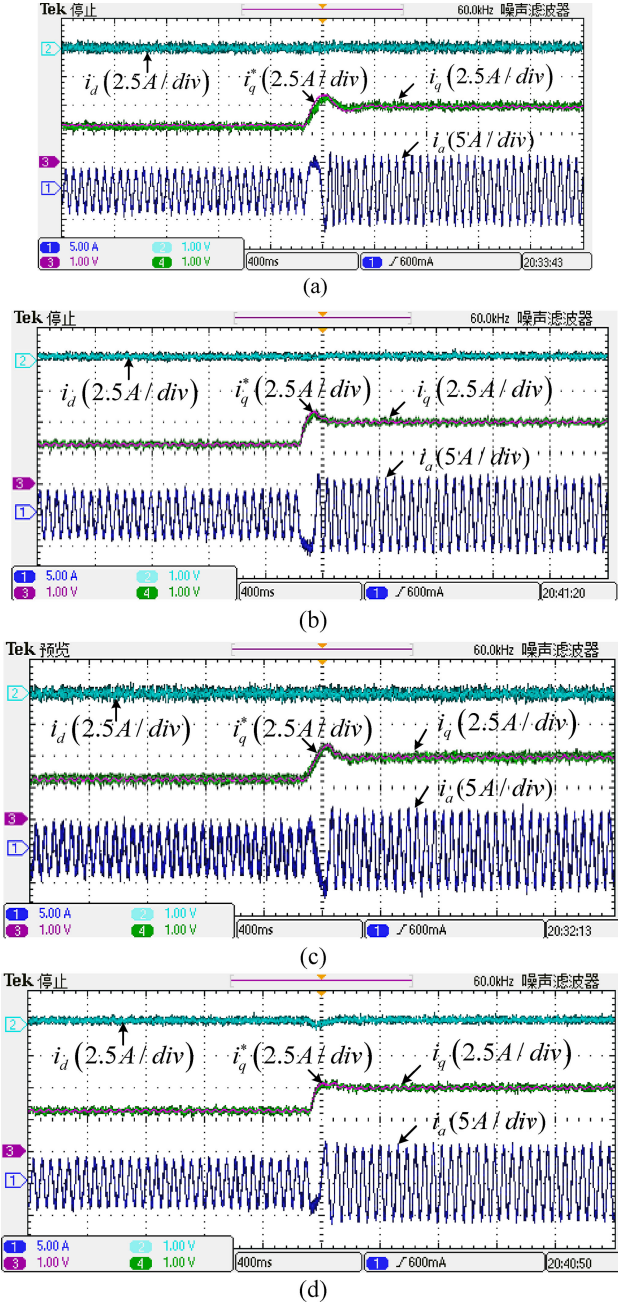


Fig. 12. Experimental results of both methods with the inductance parameter mismatch. (a) Reference and response of dq -axes current and phase current under conventional MPCC (50% error in inductance). (b) Reference and response of dq -axes current and phase current under the proposed MPCC method (50% error in inductance). (c) Reference and response of dq -axes current and phase current under conventional MPCC (100% error in inductance). (d) Reference and response of dq -axes current and phase current under the proposed MPCC method (100% error in inductance).

The experimental results of the proposed method and conventional method are shown in Figs. 10–13. The model parameters of both methods used in the experiment are listed in Table II, in which T_L represents the load torque. In addition, the PI parameters of the speed controller are designed as $K_{sp} = 0.003$ and $K_{si} = 0.001$. Fig. 10 shows the current responses of both methods with no parameter mismatch occurring. It can be seen

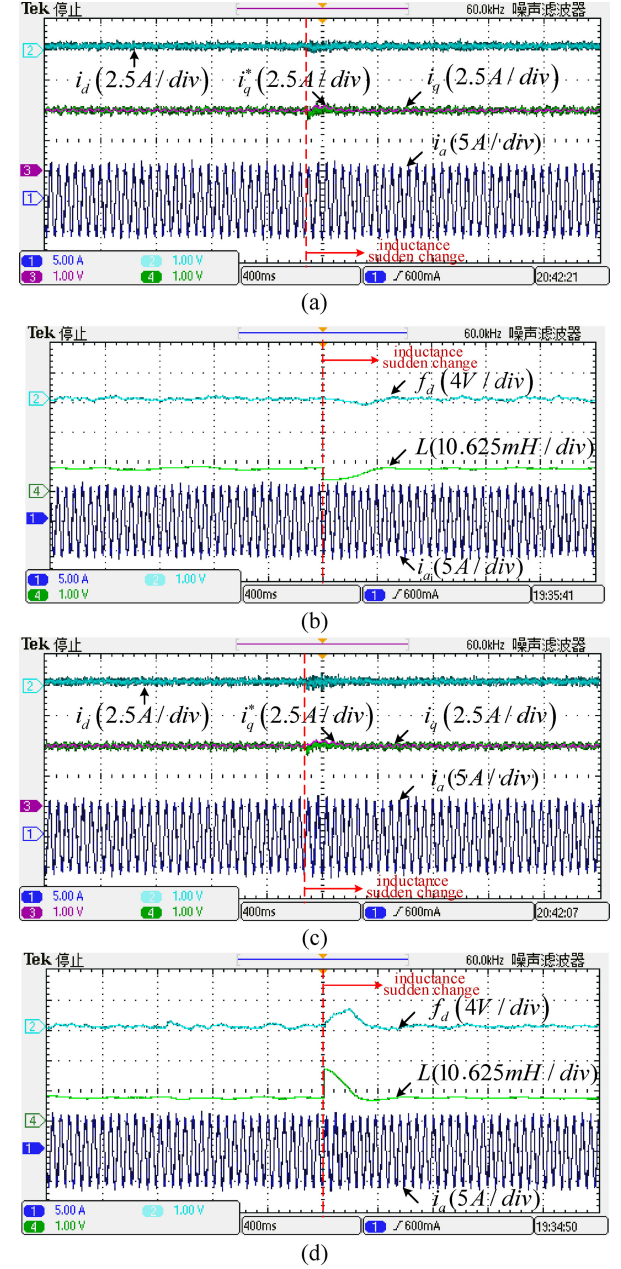


Fig. 13. Experimental results of the proposed MPCC method when inductance parameter sudden change. (a) Reference and response of dq -axes current and phase current when inductance parameter sudden decreases 50%. (b) Estimated disturbance value of the observer and inductance parameter in the model when inductance parameter sudden decreases 50%. (c) Reference and response of dq -axes current and phase current when inductance parameter sudden increases 100%. (d) Estimated disturbance value of the observer and inductance parameter in the model when inductance parameter sudden increases 100%.

that the proposed method and conventional method both have satisfactory control performances. Comparison results of both methods are shown in Fig. 11 when resistance parameter mismatch exists. Under the control of the conventional method, the existence of the resistance mismatch will lead to the current tracking error, which deteriorates the control performance of the whole control system. However, the control performance of

TABLE II
MODEL PARAMETER COMPARISON OF BOTH METHODS IN THE EXPERIMENT

	Fig.10(a) Fig.10(b)	Fig.11(a) Fig.11(b)	Fig.11(c) Fig.11(d)	Fig.12(a) Fig.12(b)	Fig.12(c) Fig.12(d)	Fig.13(a) Fig.13(b)	Fig.13(c) Fig.13(d)
$R(\Omega)$	3.18	6.36	1.59	3.18	3.18	3.18	3.18
$L(mH)$	8.5	8.5	8.5	17.0	4.25	Change from 8.5 to 17	Change from 8.5 to 4.25
$T_L(N.m)$	Change from 4 to rated value 6	Rated value 6	Rated value 6				

the proposed method has no obvious change when resistance parameter mismatch occurs. It further proves that the proposed method is not sensitive to the resistance mismatch, which is consistence with the theoretical analysis result. Fig. 12 shows the experimental results of both methods under the condition of the inductance parameter mismatch. It can be seen that the control performance of the conventional method is unsatisfactory when 50% error exists in inductance. Especially, when 100% error exists in inductance, current ripple is more obvious and the steady-state current error appears under the control of the conventional method. However, this current ripple and current error are able to be effectively eliminated by the control of the proposed MPCC method.

Fig. 13 shows the control performance of the proposed method with the rated load when a sudden change of inductance parameter occurs during the operation. From the experimental results, it can be found that the disturbance observer can quickly observe the change of disturbance f_d and the inductance value can be corrected accurately. Therefore, the dq -axes current oscillation and phase current distortions are eliminated quickly, which further verify the efficiency of the proposed MPCC method.

In sum, according to the simulation and experimental results, it can be seen that parameter mismatches would deteriorate the control performance of a conventional MPCC method; however, the proposed improved method, in this paper, has a strong antidisturbance capability of parameter and can achieve better control performance.

V. CONCLUSION

An improved MPCC method is proposed in this paper and has been experimentally applied to a PMSM system. The major contributions of this study include: 1) the incremental prediction model is used to eliminate the flux-linkage parameter, and the influence mechanism of the parameter mismatches on the current prediction is analyzed; and 2) based on this incremental prediction model, an improved MPCC method is proposed, which combined with a novel disturbance controller is able to correct the inductance value in real time and effectively improve the parameter robustness of a conventional method.

REFERENCES

- [1] G. Zhang, G. Wang, D. Xu, and N. Zhao, "ADALINE-network-based PLL for position sensorless interior permanent magnet synchronous motor drives," *IEEE Trans. Power Electron.*, vol. 31, no. 2, pp. 1450–1460, Feb. 2016.
- [2] G. Wang, R. Yang, and D. Xu, "DSP-based control of sensorless IPMSM drives for wide-speed range operation," *IEEE Trans. Ind. Electron.*, vol. 60, no. 2, pp. 720–727, Feb. 2013.
- [3] T. Geyer, G. Papafotiou, and M. Morari, "Model predictive direct torque control—Part I: Concept, algorithm, and analysis," *IEEE Trans. Ind. Electron.*, vol. 56, no. 6, pp. 1894–1905, Jun. 2009.
- [4] Y. Zhang, D. Xu, J. Liu, S. Gao, and W. Xu, "Performance improvement of model-predictive current control of permanent magnet synchronous motor drives," *IEEE Trans. Ind. Appl.*, vol. 53, no. 4, pp. 3683–3695, Jul./Aug. 2017.
- [5] J. Rodriguez and P. Cortes, *Predictive Control of Power Converters and Electrical Drives*. New York, NY, USA: Wiley-IEEE Press, 2012.
- [6] V. Yaramasu, M. Rivera, B. Wu, and J. Rodriguez, "Model predictive current control of two-level four-leg inverters—Part I: Concept, algorithm, and simulation analysis," *IEEE Trans. Power Electron.*, vol. 28, no. 7, pp. 3459–3468, Jul. 2013.
- [7] W. Xie, X. Wang, F. Wang, W. Xu, R. Kennel, and D. Gerling, "Dynamic loss minimization of finite control set-model predictive torque control for electric drive system," *IEEE Trans. Power Electron.*, vol. 31, no. 1, pp. 849–860, Jan. 2016.
- [8] M. Preindl and S. Bolognani, "Model predictive direct speed control with finite control set of PMSM drive systems," *IEEE Trans. Power Electron.*, vol. 28, no. 2, pp. 1007–1015, Feb. 2013.
- [9] S. Kouro, M. A. Perez, J. Rodriguez, and A. M. Llor, "Model predictive control: MPC's role in the evolution of power electronics," *IEEE Ind. Electron. Mag.*, vol. 9, no. 4, pp. 8–21, Dec. 2015.
- [10] F. Defay, A. M. Llor, and M. Fadel, "Direct control strategy for a four-level three-phase flying-capacitor inverter," *IEEE Trans. Ind. Electron.*, vol. 57, no. 7, pp. 2240–2248, Jul. 2010.
- [11] J. D. Barros and J. F. Silva, "Multilevel optimal predictive dynamic voltage restorer," *IEEE Trans. Ind. Electron.*, vol. 57, no. 8, pp. 2747–2760, Aug. 2010.
- [12] G. Papafotiou, J. Kley, K. G. Papadopoulos, P. Bohren, and M. Morari, "Model predictive direct torque control—Part II: Implementation and experimental evaluation," *IEEE Trans. Ind. Electron.*, vol. 56, no. 6, pp. 1906–1915, Jun. 2009.
- [13] V. Yaramasu, W. Bin, S. Alepuz, and S. Kouro, "Predictive control for low-voltage ride-through enhancement of three-level-boost and NPC-converter-based PMSG wind turbine," *IEEE Trans. Ind. Electron.*, vol. 61, no. 12, pp. 6832–6843, Dec. 2014.
- [14] Y. Cho, K.-B. Lee, J.-H. Song, and Y. I. Lee, "Torque-ripple minimization and fast dynamic scheme for torque predictive control of permanent-magnet synchronous motors," *IEEE Trans. Power Electron.*, vol. 30, no. 4, pp. 2182–2190, Apr. 2015.
- [15] Z. Song, W. Chen, and C. Xia, "Predictive direct power control for three-phase grid-connected converters without sector information and voltage vector selection," *IEEE Trans. Power Electron.*, vol. 29, no. 10, pp. 5518–5531, Oct. 2014.

- [16] S. Vazquez, A. Marquez, R. Aguilera, D. Quevedo, J. I. Leon, and L. G. Franquelo, "Predictive optimal switching sequence direct power control for grid-connected power converters," *IEEE Trans. Ind. Electron.*, vol. 62, no. 4, pp. 2010–2020, Apr. 2015.
- [17] Q. Zhang, R. Min, Q. Tong, X. Zou, Z. Liu, and A. Shen, "Sensorless predictive current controlled DC–DC converter with a selfcorrection differential current observer," *IEEE Trans. Ind. Electron.*, vol. 61, no. 12, pp. 6747–6757, Dec. 2014.
- [18] V. Smidl, S. Janous, and Z. Peroutka, "Improved stability of DC catenary fed traction drives using two-stage predictive control," *IEEE Trans. Ind. Electron.*, vol. 62, no. 5, pp. 3192–3201, May 2015.
- [19] Y. Zhang and H. Yang, "Generalized two-vector-based model-predictive torque control of induction motor drives," *IEEE Trans. Power Electron.*, vol. 30, no. 7, pp. 3818–3829, Jul. 2015.
- [20] C. A. Rojas, J. Rodriguez, F. Villarroel, J. R. Espinoza, C. A. Silva, and M. Trincado, "Predictive torque and flux control without weighting factors," *IEEE Trans. Ind. Electron.*, vol. 60, no. 2, pp. 681–690, Feb. 2013.
- [21] F. Villarroel *et al.*, "Multiobjective switching state selector for finite states model predictive control based on fuzzy decision making in a matrix converter," *IEEE Trans. Ind. Electron.*, vol. 60, no. 2, pp. 589–599, Feb. 2013.
- [22] P. Cortes *et al.*, "Guidelines for weighting factors design in model predictive control of power converters and drives," in *Proc. IEEE Int. Conf. Ind. Technol.*, 2009, pp. 1–7.
- [23] X. Zhang and B. Hou, "Double vectors model predictive torque control without weighting factor based on voltage tracking error," *IEEE Trans. Power Electron.*, vol. 33, no. 3, pp. 2368–2380, Mar. 2018.
- [24] T. Geyer and D. E. Quevedo, "Performance of multistep finite control set model predictive control for power electronics," *IEEE Trans. Power Electron.*, vol. 30, no. 3, pp. 1633–1644, Mar. 2015.
- [25] T. Geyer and D. E. Quevedo, "Multistep finite control set model predictive control for power electronics," *IEEE Trans. Power Electron.*, vol. 29, no. 12, pp. 6836–6846, Dec. 2014.
- [26] A. Linder and R. Kennel, "Model predictive control for electrical drives," in *Proc. 36th IEEE Power Electron. Spec. Conf.*, Jun. 2005, pp. 1793–1799.
- [27] H. A. Young, M. A. Perez, and J. Rodriguez, "Analysis of finite-control-set model predictive current control with model parameter mismatch in a three-phase inverter," *IEEE Trans. Ind. Electron.*, vol. 63, no. 5, pp. 3100–3107, May 2016.
- [28] L. Niu, M. Yang, and D. Xu, "An adaptive robust predictive current control for PMSM with online inductance identification," *Int. Rev. Electr. Eng.*, vol. 7, no. 2, pp. 3845–3856, 2012.
- [29] C. Xia *et al.*, "Robust model predictive current control of three - phase voltage source PWM rectifier with online disturbance observation," *IEEE Trans. Ind. Informat.*, vol. 8, no. 3, pp. 459–471, Jan. 2012.
- [30] G. H. Bode, P. C. Loh, M. J. Newman, and D. G. Holmes, "An improved robust predictive current regulation algorithm," *IEEE Trans. Ind. Appl.*, vol. 41, no. 6, pp. 1720–1733, Nov./Dec. 2005.
- [31] A. Patrycjusz and M. P. Kazmierkowski, "Virtual-flux-based predictive direct power control of AC/DC converters with online inductance estimation," *IEEE Trans. Ind. Electron.*, vol. 55, no. 12, pp. 4381–4390, Dec. 2008.
- [32] X. Zhang, B. Hou, and Y. Mei, "Deadbeat predictive current control of permanent magnet synchronous motors with stator current and disturbance observer," *IEEE Trans. Power Electron.*, vol. 32, no. 5, pp. 3818–3834, May 2017.
- [33] C. K. Lin, J. T. Yu, Y. S. Lai, and H. C. Yu, "Improved model-free predictive current control for synchronous reluctance motor drives," *IEEE Trans. Ind. Electron.*, vol. 63, no. 6, pp. 3942–3953, Jun. 2016.
- [34] C. K. Lin, T. H. Liu, J. T. Yu, L. C. Fu, and C. F. Hsiao, "Model-free predictive current control for interior permanent-magnet synchronous motor drives based on current difference detection technique," *IEEE Trans. Ind. Electron.*, vol. 61, no. 2, pp. 667–681, Jun. 2014.



Xiaoguang Zhang (M'15) received the B.S. degree in electrical engineering from the Heilongjiang Institute of Technology, Harbin, China, in 2007, and the M.S. and Ph.D. degrees in electrical engineering from Harbin Institute of Technology, Harbin, in 2009 and 2014, respectively.

From 2012 to 2013, he was a Research Associate with Wisconsin Electric Machines and Power Electronics Consortium, University of Wisconsin-Madison, Madison, USA. He is currently a Distinguished Professor with the North China University of Technology, Beijing, China. He has published more than 40 technical papers in the area of motor drives. His current research interests include power electronics and electric machines drives.



Liang Zhang was born in Beijing, China, in 1993. He received the B.S. degree in electrical engineering from the North China University of Technology, Beijing, in 2015, where he is currently working toward the M.S. degree.

His current research interests include permanent-magnet synchronous motor drives.



Yongchang Zhang (M'10–SM'18) received the B.S. degree in electrical engineering from Chongqing University, Chongqing, China, in 2004, and the Ph.D. degree in electrical engineering from Tsinghua University, Beijing, China, in 2009.

From August 2009 to August 2011, he was a Postdoctoral Fellow with the University of Technology Sydney, Australia. In August 2011, he joined the North China University of Technology, Beijing, as an Associate Professor, where he is currently a Full Professor and the Director of the Inverter Technologies Engineering Research Center of Beijing. He has published more than 100 technical papers in the area of motor drives, pulsedwidth modulation, and ac/dc converters. His current research focuses on the model predictive control for power converters and motor drives.